Commentary

Consensus statement: Standardized reporting of power-producing luminescent solar concentrator performance

Chenchen Yang,[1] Harry A. Atwater,[2] Marc A. Baldo,[3] Derya Baran,[4] Christopher J. Barile,[5] Miles C. Barr,[6] Matthew Bates,[1] Moungi G. Bawendi,[7] Matthew R. Bergren,[8] Babak Borhan,[9] Christoph J. Brabec,[10,11,12] Sergio Brovelli,[13] Vladimir Bulović,[3] Paola Ceroni,[14] Michael G. Debije,[15] Jose-Maria Delgado-Sanchez,[16] Wen-Ji Dong,[17] Phillip M. Duxbury,[18] Rachel C. Evans,[19] Stephen R. Forrest,[20,21,22,23] Daniel R. Gamelin,[24] Noel C. Giebink,[25] Xiao Gong,[26] Gianmarco Griffini,[27] Fei Guo,[28] Christopher K. Herrera,[1] Anita W.Y. Ho-Baillie,[29] Russell J. Holmes,[30] Sung-Kyu Hong,[31] Thomas Kirchartz,[32,33] Benjamin G. Levine,[34] Hongbo Li,[35] Yilin Li,[36] Dianyi Liu,[37] Maria A. Loi,[38] Christine K. Luscombe,[24,39] Nikolay S. Makarov,[8] Fahad Mateen,[31] Raffaello Mazzaro,[40] Hunter McDaniel,[8] Michael D. McGehee,[41,42,43] Francesco Meinardi,[13] Amador Menéndez-Velázquez,[44] Jie Min,[45,46] David B. Mitzi,[47] Mehdi Moemeni,[9] Jun Hyuk Moon,[48] Andrew Nattestad,[49] Mohammad K. Nazeeruddin,[50] Ana F. Nogueira,[51] Ulrich W. Paetzold,[52,53] David L. Patrick,[54] Andrea Pucci,[55] Barry P. Rand,[56,57] Elsa Reichmanis,[58] Bryce S. Richards,[52,53] Jean Roncali,[59] Federico Rosei,[60] Timothy W. Schmidt,[61] Franky So,[62] Chang-Ching Tu,[63] Aria Vahdani,[9] Wilfried G.J.H.M. van Sark,[64] Rafael Verduzco,[36] Alberto Vomiero,[65,66] Wallace W.H. Wong,[67,68] Kaifeng Wu,[69] Hin-Lap Yip,[70,71] Xiaowei Zhang,[72,73] Haiguang Zhao,[74] and Richard R. Lunt[1,18,*]

SUMMARY

Fair and meaningful device performance comparison among luminescent solar concentrator-photovoltaic (LSC-PV) reports cannot be realized without a general consensus on reporting standards in LSC-PV research. Therefore, it is imperative to adopt standardized characterization protocols for these emerging types of PV devices that are consistent with other PV devices. This commentary highlights several common limitations in LSC literature and summarizes the best practices moving forward to harmonize with standard PV reporting, considering the greater nuances present with LSC-PV. Based on these practices, a checklist of actionable items is provided to help standardize the characterization/reporting protocols and offer a set of baseline expectations for authors, reviewers, and editors. The general consensus combined with the checklist will ultimately guide LSC-PV research towards reliable and meaningful advances.

Luminescent solar concentrators/collectors (LSCs) were initially introduced to reduce the use of expensive photovoltaic (PV) materials in large-scale solar deployments. LSCs have demonstrated a number of benefits in optical and power generation applications including high defect tolerance, angle independence, scalability with low manufacturing cost, improved spectral control, potential for varied aesthetics, and high visible transparency. Due to their structural simplicity, LSCs have been widely investigated by researchers across a broad spectrum of disciplines, including chemistry, electrical engineering, materials science, optics, and physics. This diversity of backgrounds is one of the greatest strengths of the LSC field. However, there is still no general consensus on reporting standards, i.e., a standardized set of parameters and protocols that would allow for meaningful device performance comparison. It is thus critical and urgent that baseline metrics of the luminescent solar concentrator-photovoltaic (LSC-PV) system mirror those established for the photovoltaic (PV) field to enable meaningful data comparisons between laboratories and between LSC-PV devices and other electrical power-producing PV technologies, as previously done with LSC devices for alternative (non-PV) application spaces.

A schematic of an LSC-PV is shown in Figure 1A: an LSC device absorbs, converts, and concentrates/collects incident solar light by means of photoluminescence (PL) of an emitting material embedded in, or coated onto, a transparent lightguide. When used to generate electrical power, LSCs are coupled with PV devices to obtain an integrated system (LSC-PV) that converts incoming light into electricity, with an extra photon absorption/re-emission step compared to conventional PV cells. As such, the complete LSC-PV system should be treated as an integrated PV device with the same figures of merits for PV performance. The power

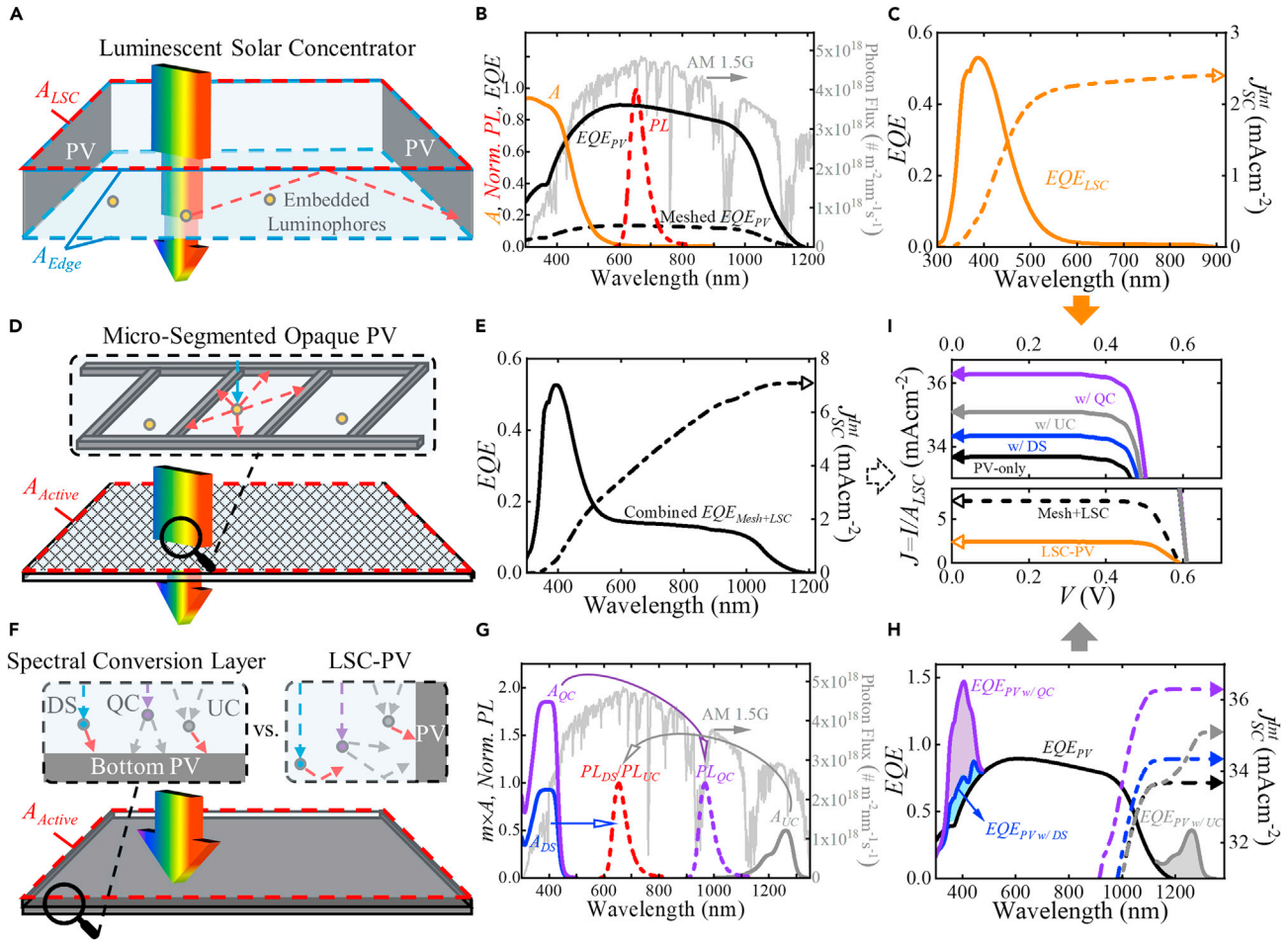

Figure 1. Various LSC-PV designs and the corresponding PV performance

(A) Schematic of an LSC-PV system. The lightguide front surface area (A_{LSC}) and total edge area (A_{Edge}) are highlighted with red and blue dashed lines, respectively. Note that the PV cells are only mounted onto the right and left lightguide edges for illustrative purpose; in real-world applications, the entire lightguide edge area would typically be mounted with PV cells for maximum output electrical power.

(B) Typical absorption (*A*, solid, in orange) and emission spectra (*PL*, dashed, in red) of luminophores for LSC-PVs with the external quantum efficiency spectrum (solid and dashed, in black) of the edge-mounted and micro-segmented PV cells (EQE_{PV}). The AM 1.5G photon flux spectrum is also included as the background (in gray).

(C) External quantum efficiency spectrum of the LSC-PV (EQE_{LSC}) resulting from the absorption, emission, and EQE_{PV} profiles shown in (B).

(D) Schematic showing the LSC lightguide embedded with micro-segmented PV, emphasizing the need to consider these systems as an integrated PV system and the inability to utilize the PV area as the active area for any *J-V* calculations.

(E) Combined $EQE_{Mesh+LSC}$ spectrum of the micro-segmented structure.

(F) Schematic showing the bottom PV cell with a top spectral conversion layer structure, which can be incorporated with various photoluminescence (PL) mechanisms including down-shifting (DS), quantum-cutting (QC) and up-conversion (UC). A conventional LSC-PV configuration with these PL mechanisms is also included for comparison.

(G) Typical absorption and emission profiles of the DS, QC, and UC PL mechanisms, where the absorption profiles are corrected by the multiplication factors (*m*, defined as the number of emitted photons per absorbed photon, and m_{DS} = 1, m_{QC} = 2, and m_{UC} = 0.5, respectively).

(H) *EQE* spectra of PVs with DS, QC, and UC spectral conversion mechanisms. The resulting *EQE* gains are highlighted in shaded colors.

(I) Current density (*J*) versus voltage (*V*) characteristics of the photovoltaic devices from (A), (D), and (F), which are used to calculate their *PCE*s based active areas (A_{LSC} or A_{Active}) highlighted with red dashed lines, respectively. The short-circuit current densities (J_{SC}) extracted from the *J-V* characteristics should match the photocurrent densities integrated from the corresponding *EQE* spectra from (C), (E), and (H), which is a critical consistency check for all photovoltaic technologies. The vertical axis of the *J-V* plot is split into two scales for visual clarity.

conversion efficiency (*PCE*) of an LSC-PV system can be calculated from the corresponding *J-V* characteristic as:

$$PCE = \frac{I_{SC} \cdot V_{OC} \cdot FF}{P_0 \cdot A_{Active}} = \frac{J_{SC} \cdot V_{OC} \cdot FF}{P_0} = \eta_{ext} \cdot \eta_{PV}^{*}$$

where I_{SC} is the short-circuit current, J_{SC} is the short-circuit current density, V_{OC} is the open-circuit voltage, *FF* is the fill factor, P_0 is the power density of the

AM 1.5G solar spectrum as the standard input intensity, A_{Active} is the active area receiving the incident solar intensity, η_{ext} is the external photon efficiency (discussed in greater detail below), and η^{*}_{PV} is the efficiency of the edge-mounted PV cell under the illumination of photoluminescence. The geometric gain G ($G = A_{LSC}/A_{Edge}$, where A_{LSC} is the LSC-PV lightguide front surface area, and A_{Edge} is the lightguide total edge area) is another design parameter. While it does not appear in the equation for calculating the *PCE*, it is important to report G alongside the *PCE* since the latter typically varies with it accordingly. If clear *J-V* hysteresis is observed in the edge-mounted PV (i.e., strong dependence on scan direction, speed, and light soaking, for example with some perovskite or dye-sensitized solar cells), monitoring of power output at maximum power point (MPP) should be considered.

The external quantum efficiency spectrum of the integrated LSC-PV system ($EQE_{LSC}(\lambda)$) is defined as the number of generated electrons by the LSC-PV system per incident photon onto the lightguide front surface at each incident wavelength, λ. The comparison of the photocurrent density extracted from *J-V* characteristic and that from the integrated *EQE* (including EQE_{LSC}) is one of the most important consistency checks for all PV technologies:

$$J_{SC}^{Int} = e \cdot \int EQE_{LSC}(\lambda) \cdot AM1.5G(\lambda) d\lambda$$

where e is the elementary charge, and the average $EQE_{LSC}(\lambda)$ should be used since it is commonly position-dependent for LSC-PVs.

Although the underlying thermodynamic theory has been established, the characterization of LSCs is surprisingly nuanced and more challenging than that of conventional PV devices. Given these circumstances, it is not surprising that confusion exists, along with a range of inconsistencies that have permeated the literature. We highlight several common errors found in the LSC literature:

(1) A number of reports have used different definitions of area to calculate the *PCE*. Since an LSC-PV device consists of a lightguide framed by PV cells, it is the LSC-PV lightguide front surface area ($A_{LSC} \equiv A_{Active}$) that receives the incident solar irradiance rather than the lightguide total edge area (A_{Edge}, for edge-mounted PV cells). Assuming no reabsorption/scattering loss within the LSC-PV system, the photocurrent (I) should be ideally proportional to the collection area A_{LSC} ($I \propto A_{LSC}$), even though in reality the scaling is sublinear. If A_{Edge} is used to calculate the *PCE*, the calculated current density ($J = I/A_{Edge}$) could exceed the values imposed by the thermodynamic limit of a PV cell if the lightguide thickness decreases with constant A_{LSC}, resulting in an overestimation of the *PCE*.

Notably, most LSC-PV systems are intrinsically bifacial, which allows illumination from both sides. The bifacial nature of the LSC-PV system is a potential benefit that can be exploited to harvest solar albedo in certain installation configurations. Diffusive and specular back reflectors can significantly increase the *PCE* up to 30% due to the double pass of light. Reverse side illumination or measurements with scatterers/reflectors can be reported but should be done so as supplemental information. Standard baseline measurements should be made with a matte black backdrop behind the test device with an air gap.

(2) Often it is only the η_{ext} that is reported for LSC-PV systems as opposed to the *J-V* characteristics, $EQE_{LSC}(\lambda)$, and *PCE*. The external photon efficiency, η_{ext}, also referred to as "optical quantum efficiency" or "optical efficiency" in some LSC reports, is commonly defined as the ratio of the total number of emitted photons reaching the lightguide edge to the total number of solar photons incident onto the lightguide front surface. However, even definitions of this seemingly simple and commonly reported parameter can vary, as they can be based on either energy flux or photon flux and have been reported at specific wavelengths or integrated across the solar spectrum. We emphasize that reporting η_{ext} based on photon flux is most relevant to the J_{SC} and *PCE* since it is a performance parameter of the purely photonic LSC lightguide, and it also directly determines the number of photogenerated carriers.

Frequently, the external photon efficiency is mistakenly calculated using $\eta_{ext} = I_{LSC}/(I_{PV} \cdot G)$, where I_{LSC} is the total short-circuit current of the LSC when PV cells are attached to all the edges and connected in parallel, and I_{PV} is the total short-circuit current of all the same edge-mounted PV cells acquired under direct illumination. This apparent concentration ratio depends critically on the spectral response of the side-mounted PV and this value is rarely corrected for spectral mismatch between the LSC absolute absorption profile and the corresponding external quantum efficiency spectra of the edge-mounted PV cells (EQE_{PV}). If the quantum efficiency of the edge-mounted PV is restricted to a specific wavelength range, this method becomes particularly erroneous (the denominator would become smaller even though the photon efficiency is the same). Since PV cells must have been mounted to make these measurements already, it is advised whenever possible to simply measure and report the *J-V* characteristic under standard illumination (the air-mass 1.5 global [AM 1.5G] spectrum under 1 sun intensity [1,000 W/m^2] at 25°C) and calculate the corresponding *PCE* based on the A_{LSC}. Photon efficiency can be obtained by measuring the LSC in an integrating sphere or by calculating from the corresponding

$EQE_{LSC}(\lambda)$. Similarly, the concentration factor (C), equal to the geometric gain corrected for efficiency losses in the LSC-PV ($C = \eta_{ext} \cdot G$), is useful in tracking whether $C > 1$ (i.e., "concentrator" versus "collector") and understanding whether the concentration function takes effect on the edge-mounted PV cells.

While the η_{ext} is insufficient to determine the device electrical power output, it is important for understanding the fundamental optical nature of purely photonic LSC devices and is a primary metric in applications where maximal electrical power production is not required. Another important parameter is the internal photon efficiency, η_{int}, which is the ratio of the number of emitted photons reaching the lightguide edge to the number of photons absorbed by the luminescent material. η_{int} is independent of both the spectral absorption width of the luminophore and the illumination source. It can be reliably obtained from integrating sphere and absorptance measurements.

(3) The EQE_{LSC} has largely been unreported in the LSC community, while it is strictly required for quantifying all PV devices. Accurate EQE_{LSC} measurements are needed to set or correct lamp intensities after mismatch factors are determined and to validate photocurrent densities from the corresponding *J-V* characteristics. The latter is particularly important for LSC-PVs, as there are a number of simplifying geometries with geometric corrections, which can potentially amplify errors. Typical absorption and emission spectra of an LSC luminophore are shown in Figure 1B, along with the EQE_{PV} of the edge-mounted PV. The EQE_{PV} spectrum should encompass the entire emission profile of the luminophore, resulting in the corresponding EQE_{LSC} as shown in Figure 1C. A series of position-dependent EQE_{LSC} spectra can provide useful information on reabsorption loss and lightguide trapping for further analysis, and any artifacts or mismeasurements, such as Rayleigh scattering centers within the LSC lightguide or direct illumination of the edge-mounted PV by uncollimated or scattered incident light beam, can be readily identified from the EQE_{LSC} profile. Therefore, by testing the position-dependent EQE_{LSC} spectra, common errors in measuring the photon efficiency can also be circumvented. Moreover, the $\eta_{ext}(\lambda)$ spectrum can be obtained from the $EQE_{LSC}(\lambda)$ profile since they are closely related:

$$EQE_{LSC}(\lambda) = \eta_{ext}(\lambda) \cdot \frac{\int EQE_{PV}(\lambda') \cdot PL(\lambda') d\lambda'}{\int PL(\lambda') d\lambda'},$$

where, to avoid confusion, the integral term is performed over the wavelength range of the PL emission (λ') rather than the wavelength of the absorption/excitation (λ). If the EQE_{PV} is flat (i.e., nearly constant) around the emission spectrum ($PL(\lambda')$), then the photon efficiency at each λ can be calculated by using $\eta_{ext}(\lambda) \cong EQE_{LSC}(\lambda)/EQE_{PV}$. Indeed, this shows how close $\eta_{ext}(\lambda)$ and $EQE_{LSC}(\lambda)$ are in definition. The overall η_{ext} can then be calculated as:

$$\eta_{ext} = \frac{\int AM\,1.5G(\lambda) \cdot \eta_{ext}(\lambda) d\lambda}{\int AM\,1.5G(\lambda) d\lambda},$$

where AM 1.5G (λ) is the photon flux spectrum in units of number of photons/(m^2-nm-s). Then η_{int} can be estimated based on η_{ext} and the corresponding absorptance profile.

Other advanced PV designs with spectral conversion mechanisms are also shown in Figure 1. For example, Figure 1D displays a schematic of the LSC with embedded micro-segmented PV (mesh), which reduces the distance to the PV cell for the emitted and lightguided PL signal, substantially lowering losses from reabsorption, which is a significant loss mechanism in conventional LSC-PV systems. The spacings between the segmented PV mesh can be adjusted to create various degrees of partial visible transparency or admittance. This design in particular highlights the problem of applying the PV area in the *J-V* measurement (as opposed to the lightguide illumination area). The A_{Active} of this structure is the entire front surface, and the meshed PV area and the lightguide front surface area become intertwined and indistinguishable. Therefore, the corresponding $EQE_{Mesh+LSC}$ profile is the combined contribution from both EQE_{Mesh} and EQE_{LSC}, as shown in Figure 1E.

Figure 1F shows a schematic of a conventional opaque PV device with a spectral conversion layer structure where down-shifting (DS), quantum-cutting (QC), and up-conversion (UC) can be incorporated into this vertical design to further enhance solar spectral utilization. The absorption and emission profiles of these PL mechanisms are shown in Figure 1G. The shaded areas in Figure 1H highlight the *EQE* gains originating from these spectral conversion mechanisms in comparison to the bare PV cell. Notably, the PV devices included in Figure 1A–1F show the progression of partial to complete PV cell coverage within the active area, which is helpful to highlight the correct collection area for *PCE* calculations.

For all the PV devices in Figure 1, the *PCE*s should always be calculated from the corresponding *J-V* characteristics acquired under a standard illumination spectrum (e.g., the air-mass 1.5 global [AM 1.5G] spectrum under 1 sun intensity [1,000 W/m^2] as shown in Figure 1I). To ensure the equivalent 1 sun intensity is applied to the *J-V* measurement of the test cells for a fair comparison between different reports (i.e., different test cell/reference cell combinations and various solar simulators with different output spectra), four spectra including the average EQE_{LSC} representing the test LSC-PV module, the *EQE* of the reference cell (this is not EQE_{PV} of the edge-mounted PV cell), the AM 1.5G spectrum, and the

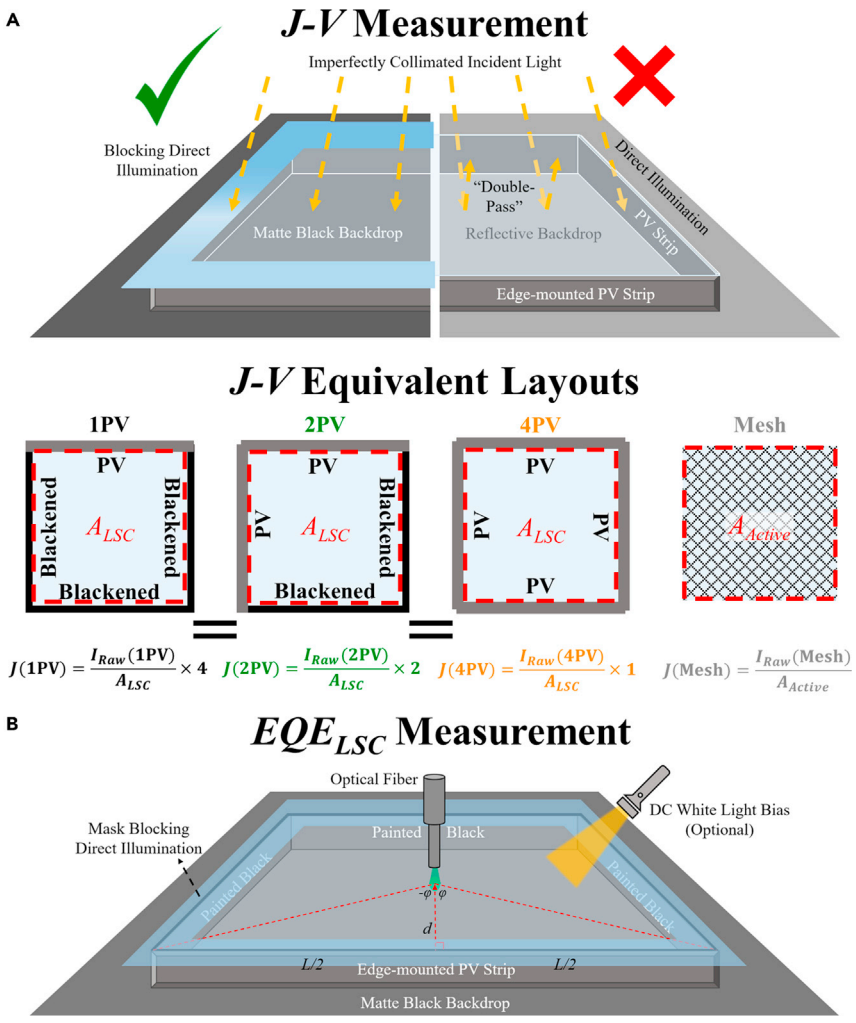

Figure 2. Key practices for LSC-PV performance characterization

(A) (Top) Schematic showing the best practices (left) of measuring the *J-V* characteristic of LSC-PV systems to avoid overestimation (right). A matte black backdrop and an opaque mask are necessary to avoid photocurrent overestimation from "double-pass" and "direct illumination" effects. Such overestimation from the raw *J-V* data can be further magnified after any geometric corrections (e.g., × 2 or × 4). (bottom) Equivalent layouts for *J-V* measurements for various square LSC-PV systems. To assure equivalence between 1, 2, and 4 cells mounting configurations, any blackened edges should be first roughened or applied with index matching gel to the blackened surface to avoid reflections. The square shape is the most common lightguide geometry, but other geometries are also acceptable with appropriate geometric corrections. The active areas (A_{LSC} = A_{Active}) are all highlighted with red dashed lines.

(B) Schematic showing the best practice setup for EQE_{LSC} measurement with a (recommended) mask around the edge. The mask is important if there is any stray chopped light, strongly divergent monochromatic beam, or if geometric correction is required. Because of typical reabsorption losses, the EQE_{LSC} is position-dependent. Thus, it is necessary to determine an average EQE_{LSC} as the representative for integration of the J_{SC} (J_{SC}^{Int}). For measurements with a single mounted PV, three edges without PVs should be painted black to allow for geometric correction (e.g., $g = (\pi/\tan^{-1}(L/2d))$, where L is the lightguide length and d is the centerline distance between the excitation beam and the edge-mounted PV cell, should be applied for each raw EQE_{LSC} spectrum acquired at each centerline position, d). We encourage the use of LSCs with $L \geq 5$ cm for this test, which can effectively minimize errors originating from direct illumination of the edge-mounted PV by imperfectly collimated or scattered incident light beam. No correction (either for *J-V* or EQE_{LSC} measurement) is needed if all edges are PV mounted or a mesh PV is utilized, and such corrections are not typical for third-party certifications since the full device integration/wiring are usually

output spectrum of the solar simulator should be used to determine the corresponding spectral mismatch factor (M), which can then be applied to set the solar simulator with the correct illumination intensity.

To validate these measurements, it is critical to compare the photocurrent density extracted from *J-V* characteristics (J_{SC}, Figure 1I) and that integrated from the average *EQE* (J_{SC}^{Int}, Figure 1C, E and H) to confirm that these match within experimental error. This consistency check is even more crucial with LSC-PVs because of the greater number of possible ways to err in measuring or calculating *Jsc*.

(4) Confusion around the "concentration" function and impact persists with some claims of EQE_{LSC} > 100% in the absence of multi-exciton generation (MEG), singlet fission, QC, etc. Without such phenomena, a maximum of one incident photon on the lightguide can be absorbed, re-emitted and light-guided to generate one electron-hole pair in the edge-mounted PV, so that both EQE_{LSC} and η_{ext} are $\lesssim$100%. In contrast, the concentration factor, C, which measures the actual "concentration" or flux gain, has no theoretical upper bound.

In summary, we have highlighted the main issues that have made it difficult to compare results and assess progress in the field of LSC-PVs designed primarily for electrical power generation. Recently, standard protocols for measuring the performance of PVs, electrical power producing LSC-PVs, and photonic LSCs have been outlined.

Figure 2. *Continued*

required. Application of a DC white light bias is also recommended to better mimic the overall photon and carrier density during the test and is particularly important for PL mechanisms with nonlinear light intensity dependence such as UC and when the edge-mounted PV exhibits nonlinear light intensity dependence.

Key practices for LSC-PV performance characterization are graphically summarized in Figure 2. Here, we adapt these protocols to develop an LSC-PV checklist (Table S1: "checklist for power-producing luminescent solar concentrator manuscripts") that is analogous to, yet more nuanced than the "standardized data reporting for photovoltaic cells" by Cell Press, in terms of more consistency validation checks and detailed protocols to minimize inaccuracies. To help the community reliably report performance metrics and alleviate concerns over experimental errors and conceptual mistakes in LSC-PV research, we encourage authors to provide the details from the LSC-PV checklist in their submitted research articles. As an added benefit, such reporting will enable inclusion of the reported data to the "Reporting Device Efficiency of Emerging PV Materials" database. We also encourage authors to submit their LSC-PVs for third-party certification when claiming record values of efficiency. We hope that the use of this checklist will become standard for all LSC-PV reports, allowing published results to be readily comparable between reports (among LSC-PV reports, and between LSC-PV and other PV technologies). We emphasize that adopting the metrics outlined in this checklist will help the community achieve its goal of accelerating reproducible and robust advances in the development of LSC-PV devices.

Finally, we refer readers to the following literature, which describes the theoretical and practical efficiency limits of LSC-PV systems, standard characterization and reporting protocols, necessary data validation and consistency checks for PVs and LSC-PVs, and standard procedures to determine the mismatch factor. These references also highlight the potential errors that may occur along with effective approaches for their avoidance.[1–13] We also refer readers to the following literature, which describes the recommended characterization and reporting protocols for determination of the performance of LSCs as photonic systems. Common sources of error and suggestions for how these should be avoided are also provided, and the characterization of long-term performance of LSCs is also included.[14,15]

SUPPLEMENTAL INFORMATION

Supplemental information can be found online at https://doi.org/10.1016/j.joule.2021.12.004.

ACKNOWLEDGMENTS

C.Y. and R.R.L. acknowledge financial support under National Science Foundation grant CBET-1702591. D.R.G. thanks the National Science Foundation (DMR-1719797) for support. A.H.-B. is supported by the Australian Research Council (ARC) Future Fellowship FT210100210. F.R. is grateful to the Canada Research Chairs program for partial salary support. A. Vomiero acknowledges financial support from the Kempe Foundation and the Knut & Alice Wallenberg Foundation.

DECLARATION OF INTERESTS

M.C.B. (CTO), V.B., and R.R.L. are founders and non-majority owners of Ubiquitous Energy, Inc., a company working to commercialize TPV and TLSC technologies. H.M. (CEO) is a founder and non-majority owner of UbiQD, Inc., a company working to commercialize LSC and TLSC technologies. M.R.B and N.S.M. are non-majority owners of UbiQD, Inc. D.R.G. is a founder and non-majority owner of BlueDot Photonics, Inc., a company working to commercialize QC spectral-downconversion PV technologies. F. Meinardi is a founder and non-majority owner of Glass to Power SpA, a company working to commercialize LSC technologies.

1. EPVRI. Emerging PV. https://emerging-pv.org/.
2. Almora, O., Baran, D., Bazan, G.C., Berger, C., Cabrera, C.I., Catchpole, K.R., Erten-Ela, S., Guo, F., Hauch, J., Ho-Baillie, A.W.Y., et al. (2021). Device Performance of Emerging Photovoltaic Materials (Version 1). Adv. Energy Mater. *11*, 2002774.
3. Roncali, J. (2020). Luminescent Solar Collectors: Quo Vadis? Adv. Energy Mater. *10*, 2001907.
4. Yang, C., Liu, D., Bates, M., Barr, M.C., and Lunt, R.R. (2019). How to Accurately Report Transparent Solar Cells. Joule *3*, 1803–1809.
5. Yang, C., Liu, D., and Lunt, R.R. (2019). How to Accurately Report Transparent Luminescent Solar Concentrators. Joule *3*, 2871–2876.
6. Bergren, M.R., Makarov, N.S., Ramasamy, K., Jackson, A., Guglielmetti, R., and McDaniel, H. (2018). High-Performance $CuInS_2$ Quantum Dot Laminated Glass Luminescent Solar Concentrators for Windows. ACS Energy Lett. *3*, 520–525.
7. Mazzaro, R., and Vomiero, A. (2018). The Renaissance of Luminescent Solar Concentrators: The Role of Inorganic Nanomaterials. Adv. Energy Mater. *8*, 1801903.
8. Yang, C., and Lunt, R.R. (2017). Limits of Visibly Transparent Luminescent Solar Concentrators. Adv. Opt. Mater. *5*, 1600851.
9. Rau, U., Paetzold, U.W., and Kirchartz, T. (2014). Thermodynamics of light management in photovoltaic devices. Phys. Rev. B *90*, 035211.
10. Zimmermann, E., Ehrenreich, P., Pfadler, T., Dorman, J.A., Weickert, J., and Schmidt-Mende, L. (2014). Erroneous efficiency reports harm organic solar cell research. Nat. Photonics *8*, 669–672.
11. Snaith, H.J. (2012). The perils of solar cell efficiency measurements. Nat. Photonics *6*, 337–340.
12. Snaith, H.J. (2012). How should you measure your excitonic solar cells? Energy Environ. Sci. *5*, 6513–6520.
13. Shrotriya, V., Li, G., Yao, Y., Moriarty, T., Emery, K., and Yang, Y. (2006). Accurate Measurement and Characterization of Organic Solar Cells. Adv. Funct. Mater. *16*, 2016–2023.
14. Debije, M.G., Evans, R.C., and Griffini, G. (2021). Laboratory protocols for measuring and reporting the performance of luminescent solar concentrators. Energy Environ. Sci. *14*, 293–301.
15. Papakonstantinou, I., Portnoi, M., and Debije, M.G. (2021). The Hidden Potential of Luminescent Solar Concentrators. Adv. Energy Mater. *11*, 2002883.

[1]Department of Chemical Engineering and Materials Science, Michigan State University, East Lansing, MI 48824, USA

[2]Applied Physics and Kavli Nanoscience Institute, California Institute of Technology, Pasadena, CA 91125, USA

[3]Department of Electrical Engineering and Computer Science, Massachusetts Institute of Technology, Cambridge, MA 02139, USA

[4]King Abdullah University of Science and Technology (KAUST), Division of Physical Sciences and Engineering (PSE), KAUST Solar Center (KSC), Thuwal 23955, Saudi Arabia

[5]Department of Chemistry, University of Nevada, Reno, NV 89557-0216, USA

[6]Ubiquitous Energy, Inc., Redwood City, CA 94063, USA

[7]Department of Chemistry, Massachusetts Institute of Technology, Cambridge, MA 02139, USA

[8]UbiQD, Inc. Los Alamos, NM 87544, USA

[9]Department of Chemistry, Michigan State University, East Lansing, MI 48824, USA

[10]Institute Materials for Electronics and Energy Technology (i-MEET) Department for Material Science, Friedrich-Alexander Universität Erlangen-Nürnberg (FAU), 91054 Erlangen, Germany

[11]Zernike Institute for Advanced Materials, University of Groningen Nijenborgh 4, Groningen, AG NL-9747, the Netherlands

[12]High Throughput Research in PV, IEK-11, Helmholtz Institute Erlangen-Nürnberg (HIERN), Forschungszentrum Jülich, 91054 Erlangen, Germany

[13]Dipartimento di Scienza dei Materiali, Università degli Studi di Milano-Bicocca, via Cozzi 55, 20125, Milano, Italy

[14]Chemistry Department "Giacomo Ciamician," University of Bologna, 40126, Bologna, Italy

[15]Department Chemical Engineering and Chemistry, Eindhoven University of Technology, 5600 MB Eindhoven, the Netherlands

[16]Department of Applied Physics, University of Seville, Avda Reina Mercedes s/n, Seville, Spain

[17]The Gene and Linda Voiland School of Chemical Engineering and Bioengineering, Washington State University, Pullman, WA 99164, USA

[18]Department of Physics and Astronomy, Michigan State University, East Lansing, MI 48824, USA

[19]Department of Materials Science & Metallurgy, University of Cambridge, Cambridge, UK

[20]Applied Physics Program, University of Michigan, Ann Arbor, MI 48109, USA

[21]Department of Electrical Engineering and Computer Science, University of Michigan, Ann Arbor, MI 48109, USA

[22]Department of Physics, University of Michigan, Ann Arbor, MI 48109, USA

[23]Department of Material Science and Engineering, University of Michigan, Ann Arbor, MI 48109, USA

[24]Department of Chemistry, University of Washington, Seattle, WA 98195-1700, USA

[25]Department of Electrical Engineering, The Pennsylvania State University, University Park, PA 16802, USA

[26]State Key Laboratory of Silicate Materials for Architectures, Wuhan University of Technology, Wuhan 430070, China

[27]Department of Chemistry, Materials and Chemical Engineering "Giulio Natta," Politecnico di Milano, Italy

[28]Institute of New Energy Technology, College of Information Science and Technology, Jinan University, Guangzhou 510632, China

[29]School of Physics and The University of Sydney Nano Institute, The University of Sydney, Sydney, NSW 2006, Australia

[30]Department of Chemical Engineering and Materials Science, University of Minnesota, Minneapolis, MN 55455, USA

[31]Department of Chemical and Biochemical Engineering, Dongguk University, Seoul 04620, Republic of Korea

[32]IEK5-Photovoltaics Forschungszentrum Jülich, Jülich 52425, Germany

[33]Faculty of Engineering and CENIDE University of Duisburg-Essen, Duisburg 47057, Germany

[34]Department of Chemistry and Institute for Advanced Computational Science, Stony Brook University, Stony Brook, NY 11794, USA

[35]Beijing Key Laboratory of Construction-Tailorable Advanced Functional Materials and Green Applications, Experimental Center of Advanced Materials School of Materials Science and Engineering, Beijing Institute of Technology, Beijing 100081, China

[36]Department of Chemical and Biomolecular Engineering, Rice University, Houston, TX 77005, USA

[37]School of Engineering, Westlake University, 18 Shilongshan Road, Hangzhou, Zhejiang, China

[38]Photophysics and OptoElectronics Group Zernike Institute for Advanced Materials University of Groningen Nijenborgh 4, Groningen, AG 9747, the Netherlands

[39]Materials Science and Engineering Department, University of Washington, Seattle, WA 98195, USA

[40]Physics and Astronomy Department "A. Righi," University of Bologna, 40129 Bologna, Italy

[41]National Renewable Energy Laboratory, Golden, CO 80401, USA

[42]Materials Science and Engineering, University of Colorado, Boulder, CO 80309, USA

[43]Department of Chemical and Biological Engineering, University of Colorado, Boulder, CO 80309, USA

[44]Photoactive Materials Research Unit, IDONIAL Technology Center, 33417 Avilés, Asturias, Spain

[45]The Institute for Advanced Studies, Wuhan University, Wuhan 430072, China

[46]Key Laboratory of Materials Processing and Mold (Zhengzhou University), Ministry of Education, Zhengzhou 450002, China

[47]Department of Mechanical Engineering and Material Science & Department of Chemistry, Duke University, Durham, NC 27708, USA

[48]Department of Chemical and Biomolecular Engineering, Sogang University, 35 Baekbeom-ro, Mapo-gu, Seoul 04107, Republic of Korea

[49]School of Chemistry, Monash University, Clayton, VIC 3800, Australia

[50]Group for Molecular Engineering and Functional Materials, Ecole Polytechnique Fédérale de Lausanne, Institut des Sciences et Ingénierie Chimiques, Sion CH-1951, Switzerland

[51]Chemistry Institute, University of Campinas, PO Box 6154, Campinas, São Paulo 13083-970, Brazil

[52]Karlsruhe Institute of Technology, Institute of Microstructure Technology, Hermann-von-Helmholtz-Platz 1, 76344 Eggenstein-Leopoldshafen, Germany

[53]Karlsruhe Institute of Technology, Light Technology Institute, Engesserstrasse 13, 76131 Karlsruhe, Germany

[54]Department of Chemistry, Western Washington University, 516 High Street, Bellingham, WA 98225, USA

[55]Dipartmento di Chimica e Chimica Industriale, Università di Pisa, Via Moruzzi 13, 56124 Pisa, Italy

[56]Department of Electrical and Computer Engineering, Princeton University, Princeton, NJ 08544, USA

[57]Andlinger Center for Energy and the Environment, Princeton University, Princeton, NJ 08544, USA

[58]Department of Chemical and Biomolecular Engineering, Lehigh University, 111 Research Drive, Bethlehem, PA 18015, USA

[59]Supramolecular Organic and Organometallic Chemistry Center, Babes-Bolyai University, 11 Arany Janos str., 400028 Cluj-Napoca, Romania

[60]Institut National de la Recherche Scientifique INRS-Énergie, Matériaux et Télécommunications, 1650 Blvd. Lionel-Boulet, Varennes, QC J3X 1S2, Canada

[61]ARC Centre of Excellence in Exciton Science, School of Chemistry, UNSW, Sydney, NSW, Australia

[62]Department of Materials Science and Engineering, North Carolina State University, Raleigh, NC 27695, USA

[63]University of Michigan-Shanghai Jiao Tong University Joint Institute, Shanghai Jiao Tong University, Shanghai 200240, China

[64]Copernicus Institute of Sustainable Development, Utrecht University, Princetonlaan 8a, 3584CB Utrecht, the Netherlands

[65]Department of Molecular Sciences and Nanosystems, Ca' Foscari University of Venice, Via Torino 155, 30172 Venezia Mestre, Italy

[66]Division of Material Science, Department of Engineering Sciences and Mathematics, Luleå University of Technology, 971 87 Luleå, Sweden

[67]ARC Centre of Excellence in Exciton Science, The University of Melbourne, Parkville, VIC 3010, Australia

[68]School of Chemistry, The University of Melbourne, Parkville, VIC 3010, Australia

[69]State Key Laboratory of Molecular Reaction Dynamics, Dalian Institute of Chemical Physics, Chinese Academy of Sciences, Dalian, Liaoning 116023, China

[70]State Key Laboratory of Luminescent Materials and Devices, South China University of Technology, Guangzhou 510641, China

[71]Department of Materials Science and Engineering, School of Energy and Environmental Science, City University of Hong Kong, Kowloon, Hong Kong

[72]Department of Electrical Engineering and Computer Science, Ningbo University, Ningbo 315211, China

[73]National Laboratory of Solid State Microstructures, Nanjing University, Nanjing 210093, China

[74]State Key Laboratory of Bio-Fibers and Eco-Textiles & College of Physics, University-Industry Joint Center for Ocean Observation and Broadband Communication, Qingdao University, No. 308 Ningxia Road, Qingdao 266071, P.R. China

*Correspondence: rlunt@msu.edu

https://doi.org/10.1016/j.joule.2021.12.004